

# Wave-equation migration velocity analysis using extended images

Tongning Yang\* and Paul Sava, *Center for Wave Phenomena, Colorado School of Mines*

## SUMMARY

Wave-equation migration velocity analysis (WEMVA) is a velocity estimation technique designed to invert for velocity information using migrated images. Its capacity for handling multi-pathing makes it appropriate in complex subsurface regions characterized by strong velocity variation. WEMVA operates by establishing a linear relation between a velocity model perturbation and a corresponding migrated image perturbation. The linear relationship is derived from conventional extrapolation operators and it inherits the main properties of frequency-domain wavefield extrapolation. A key step in implementing WEMVA is to design an appropriate procedure for constructing image perturbations. Using time-lag extended images, one can characterize the error in migrated images by defining the focusing error as the shift of the focused reflection along the time-lag axis. Under the linear approximation, the focusing error can be transformed into an image perturbation by multiplying it with an image derivative taken relative to the time-lag parameter. The resulting image perturbation is thus a mapping of the velocity error in image space. This approach is computationally efficient and simple to implement, and no further assumptions about smoothness and homogeneity of the velocity model and reflector geometry are needed. Synthetic examples demonstrate the successful application of our method to a complex velocity model.

## INTRODUCTION

In regions characterized by complex subsurface structure, wave-equation depth migration is a powerful tool for accurately imaging the earth's interior. However, the quality of the final image greatly depends on the quality of the velocity model, thus constructing accurate velocity is essential for imaging.

Based on the domain in which the velocity estimation is implemented, velocity analysis techniques can be roughly divided into two categories. The first category includes techniques developed in the data domain prior to migration and usually described as tomography. The input for this type of techniques is the recorded seismic data. Velocity update is achieved by adjusting the velocity model to minimize the difference between the recorded and predicted seismograms. The second category includes techniques developed in the image domain after migration and usually described as migration velocity analysis (MVA). The input for this type of techniques is the migrated image obtained using an approximation of the velocity model. Velocity update is performed by adjusting the velocity model to optimize certain properties of the images, e.g. by using focusing or semblance analysis.

In practice, there are many possible approaches to employ the techniques in the two categories mentioned here. However, all such realizations share a common element that they need

a carrier of information to connect the input data or image to the output velocity model. Thus the techniques for velocity updates can also be divided into two categories as ray-based and wave-based methods. The first category refers to techniques which use wide-band rays as the information carrier (Bishop et al., 1985; Stork and Clayton, 1991). By contrast, the second category refers to techniques which use band-limited wavefields as the information carrier (Woodward, 1992; Pratt, 1999; Sirgue and Pratt, 2004). Generally speaking, ray-based methods have the advantages of simple implementation and efficient computation over wave-based methods. On the other hand, wave-based methods are capable of handling complicated wave propagation phenomena, which always happen in complex subsurface regions. Therefore, they are more robust and consistent with the wave-based migration techniques used in such regions. In this paper, the focus is on the wave-based migration velocity analysis method known as wave-equation MVA (Sava and Biondi, 2004a,b; Albertin et al., 2006; Sava and Vlad, 2008).

For the implementation of WEMVA, one important component is the construction of an image perturbation which is linked linearly to a slowness perturbation. To construct the image perturbation, measurement of the quality of migrated images must be performed first. Sava and Biondi (2004b) discuss several types of measurement for the error contained in migrated images, for example, focusing analysis (MacKay and Abma, 1992; Lafond and Levander, 1993) and moveout analysis (Yilmaz and Chambers, 1984; Biondi and Sava, 1999). For the construction of image perturbation, the most common approach is to compare a reference image with an improved version of it. The image-comparison approach has at least two drawbacks. First, the improved version of the image is always obtained by remigration with one or more models, which is computationally expensive. Second, if the reference image is incorrectly constructed, the difference between two images can exceed the small perturbation assumption, which leads to the cycle skipping problem. An alternative to this approach, discussed in Sava (2003), uses prestack Stolt migration to construct a linearized image perturbation. This alternative approach avoids the cycle skipping problem, but suffers from the approximation embedded in the underlying Stolt migration.

Focusing analysis information can be extracted from time-lag extended images (Sava and Fomel, 2006). The focusing error is measured along the time-lag axis and quantified as the departure of the focusing time-lag from zero. Higginbotham and Brown (2008) propose a method to convert this focusing error into velocity updates for the background model. However, this approach uses vertical updates of the measured errors which may fail in complex environments.

In this paper, we propose a new methodology for constructing image perturbations based on the time-lag extended imaging condition and focusing analysis. We demonstrate that the image perturbation can be easily calculated by a simple multipli-

## Time-lag extended image perturbation

cation of image derivatives and measured focusing errors. We also demonstrate that this type of image perturbation is fully consistent with the linearization embedded in WEMVA. We illustrate our method by applying the technique to the complex Sigsbee 2A model.

### THEORY

Under the single scattering approximation, seismic migration consists of two steps: wavefield reconstruction followed by the application of an imaging condition. We commonly discuss about a ‘‘source’’ wavefield, originating at the seismic source and propagating in the medium prior to any interaction with the reflectors, and a ‘‘receiver’’ wavefield, originating at discontinuities and propagating in the medium to the receivers (Berkhout, 1982). The two wavefields are kinematically equivalent at discontinuities. Any mismatch between the wavefields indicates inaccurate wavefield reconstruction typically assumed to be due to inaccurate velocity. The source and receiver wavefields can be represented as four-dimensional objects function of position  $\mathbf{x} = (x, y, z)$  and frequency  $\omega$ ,

$$u_s = u_s(\mathbf{x}, \omega), \quad (1)$$

$$u_r = u_r(\mathbf{x}, \omega). \quad (2)$$

An imaging condition is designed to extract from these extrapolated wavefields the locations where reflectors occur in subsurface. A conventional imaging condition (Claerbout, 1985) forms an image as the zero cross-correlation lag between the source and receiver wavefields:

$$r(\mathbf{x}) = \sum_{\omega} u_r(\mathbf{x}, \omega) u_s^*(\mathbf{x}, \omega), \quad (3)$$

where  $r$  is the image of subsurface and  $*$  represents complex conjugation. An extended imaging condition (Sava and Fomel, 2006) extracts the image by cross-correlation between the wavefields shifted by the time-lag  $\tau$ :

$$r(\mathbf{x}, \tau) = \sum_{\omega} u_r(\mathbf{x}, \omega) u_s^*(\mathbf{x}, \omega) e^{2i\omega\tau}. \quad (4)$$

When the model used for imaging is erroneous, the images are formed incorrectly. In the hypercube of time-lag extended images, this incorrect imaging is equivalent to a shift of focusing from zero to nonzero time-lags. Therefore, we can measure the difference between the time-lag at which the reflection focus and the zero axis and define it as the quantity  $\Delta\tau$ , which we label as time-lag perturbation to be exploited for MVA. Furthermore, we can generalize the WEMVA operators constructed for conventional imaging condition (Sava and Vlad, 2008) to include this type of image extension.

We can characterize the true slowness model as a sum of the background slowness  $s_b$  with a slowness perturbation  $\Delta s$ ,

$$s(\mathbf{x}) = s_b(\mathbf{x}) + \Delta s(\mathbf{x}). \quad (5)$$

Accordingly, the image can also be characterized as a sum between the background image  $r_b$  and an image perturbation  $\Delta r$ :

$$r(\mathbf{x}) = r_b(\mathbf{x}) + \Delta r(\mathbf{x}). \quad (6)$$

The perturbation  $\Delta s$  and  $\Delta r$  are linearly related by the WEMVA operator  $\mathbf{L}$ :

$$\Delta r = \mathbf{L}\Delta s. \quad (7)$$

Since the information of  $\Delta\tau$  is available from measurements performed on time-lag extended images, we can construct image perturbation by a linearization of the image relative to the time-lag parameter:

$$\Delta r(\mathbf{x}, \tau) = \frac{\partial r(\mathbf{x}, \tau)}{\partial \tau} \Delta\tau, \quad (8)$$

where the extended image derivative with respect to time-lag  $\tau$  is

$$\frac{\partial r(\mathbf{x}, \tau)}{\partial \tau} = \sum_{\omega} (2i\omega) u_r(\mathbf{x}, \omega) u_s^*(\mathbf{x}, \omega) e^{2i\omega\tau}. \quad (9)$$

Notice that the construction of the extended image derivative requires the same procedure as the one used for constructing the extended images. The additional term  $2i\omega$  acts as a scaling factor applied at each frequency.

In summary, we construct the image perturbations for use in connection with WEMVA using the following procedure:

- Migrate the image and output time-lag extended images according to equation 4;
- Measure  $\Delta\tau$  on time-lag panels by direct picking;
- Construct the extended image derivatives according to equation 9;
- Construct the linearized image perturbation according to equation 8.

Our methodology has the advantage over the method of Sava and Biondi (2004a,b) that we do not need to make assumptions about the slowness background as is required by the linearized Stolt procedure. Furthermore, our method does not assume horizontal reflectors, as required by conventional depth-focusing analysis technique. Our method also maintains a low computational cost, since the calculation of the linearized image perturbation, equation 8, adds just a trivial cost to that of conventional migration. Overall, our approach provides an efficient way to construct image perturbations consistent with the assumptions made about the WEMVA operator.

### EXAMPLE

We illustrate our procedure using the Sigsbee 2A model (Paffenholz et al., 2002). For simplicity, we consider just one reflector of the model in order to highlight the behavior of our operator (Figures 1(a)-1(c)). Given the linear nature of the imaging process, more reflectors contribute independently to the velocity update. We use a scaled version of the true model as the background slowness model for migration with extended images. We refer to the difference between the true and background slowness models as the true slowness perturbation  $\Delta s$ . Figures 1(b) and 1(c) show the image and time-lag extended images migrated with the background slowness model. The reflector is mispositioned due to the incorrect slowness model.

## Time-lag extended image perturbation

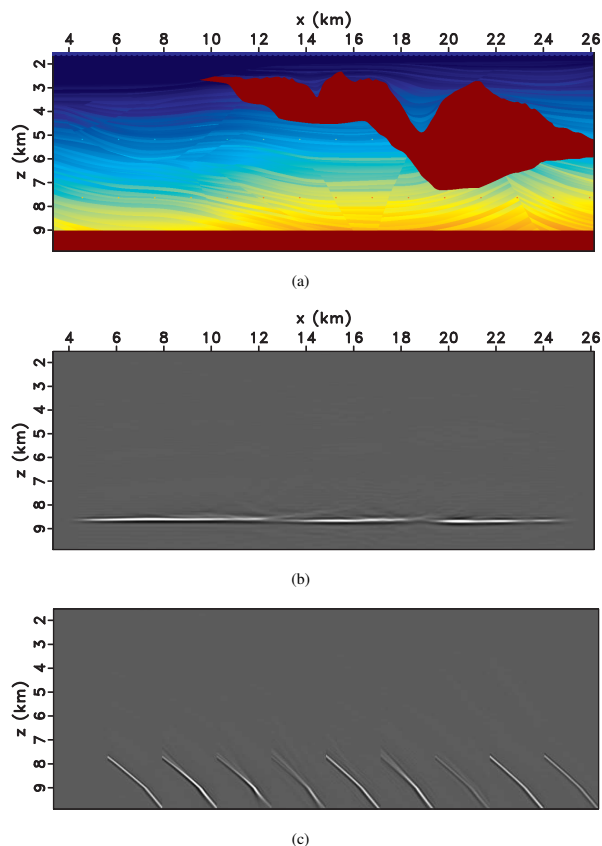


Figure 1: (a) Sigsbee 2A synthetic model, (b) migrated image corresponding to the horizontal reflectors at the bottom of the model and (c) time-lag CIGs corresponding to the background slowness at several locations in the image. Each event corresponds to a time-lag CIG just as the one shown in panel 2(a)

Figure 2(a) and 2(b) show the time-lag CIG and the constructed  $\Delta\tau$  panel obtained by picking  $\Delta\tau$  on panel 2(a) and by spreading that information evenly along the corresponding reflector. Then we construct the image perturbation by the procedure discussed in the preceding section.

To verify the accuracy of the constructed image perturbation, we apply the forward WEMVA operator to the true slowness perturbation and obtain the true image perturbation. Figures 3(c) and 3(d) depict the image perturbations obtained by the forward WEMVA operator and our method, respectively. The two images are similar both kinematically and dynamically. We apply the adjoint WEMVA operator to both image perturbations to obtain slowness perturbations shown in Figures 3(a) and 3(b), which also exhibit good similarity. Therefore, we conclude that the image perturbation constructed by our method is applicable to WEMVA since it matches the corresponding perturbations.

Figures 4(a) to 4(e) depict the slowness perturbation back-projected from the constructed image perturbation for different shots, and Figure 4(f) depicts the result of slowness perturbation stacked for all shots. The images show that the illumi-

nation pattern of the various shots is different, although consistent with the illumination of the corresponding migration procedure.

This example demonstrates that our procedure is applicable to a shot-record imaging framework in complex media. This conclusion makes our technique particularly attractive for MVA using wide-azimuth data. However, there is no particular limitation of the type of carrier used to transfer the time-lag information measured on the migrated images into velocity updates. We could, in principle, use plane waves instead of shots as information carrier, thus achieving even higher computational efficiency.

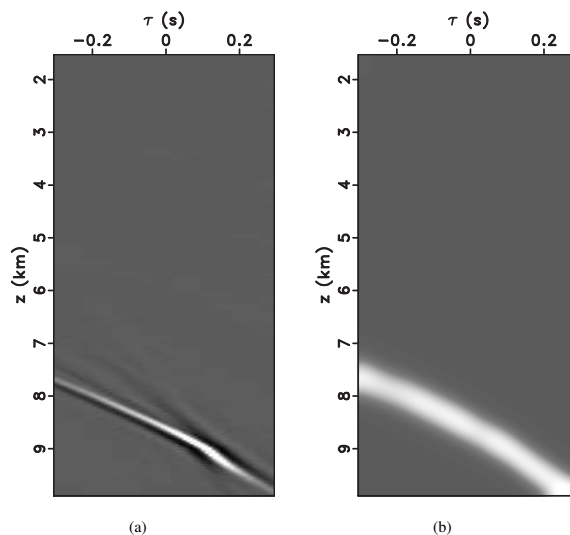


Figure 2: (a) Time-lag CIG panel at  $x = 10.1$  km and (b) picked time-lag perturbation spread along the corresponding reflector.

## CONCLUSIONS

We develop a new method to construct image perturbations for wave-equation migration velocity analysis. The methodology relies on the focusing information extracted from time-lag extended images. The shift of the reflection focusing along the time-lag axis provides a measure of error. We use this information in conjunction with image derivatives relative to the time-lag parameter to construct image perturbations. Compared with more conventional techniques for constructing image perturbations, our approach is efficient, since it represents a relatively trivial extension of the time-lag extended imaging condition, and accurate, since it does not make use of Stolt-like procedures which incorporate strong assumptions about the smoothness of the background model. The results obtained using the complex Sigsbee 2A model demonstrate the validity of our method in complex environments.

## ACKNOWLEDGMENTS

We acknowledge the support of the sponsors of the Center for Wave Phenomena at Colorado School of Mines. This work is also partially supported by a research grant from StatoilHydro.

### Time-lag extended image perturbation

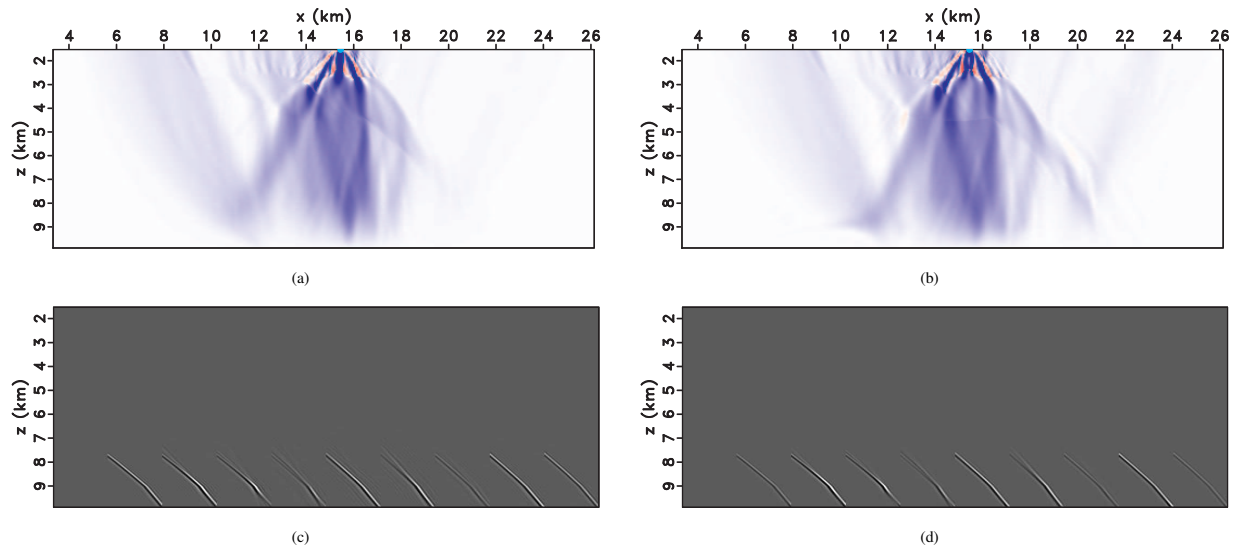


Figure 3: (a) Slowness perturbation obtained by applying the adjoint WEMVA operator to image perturbation (c). (b) Slowness perturbation obtained by applying the adjoint WEMVA operator to image perturbation (d). (c) Image perturbation obtained by applying the forward operator to the true slowness perturbation. (d) Image perturbation obtained by the linearized extended image procedure.

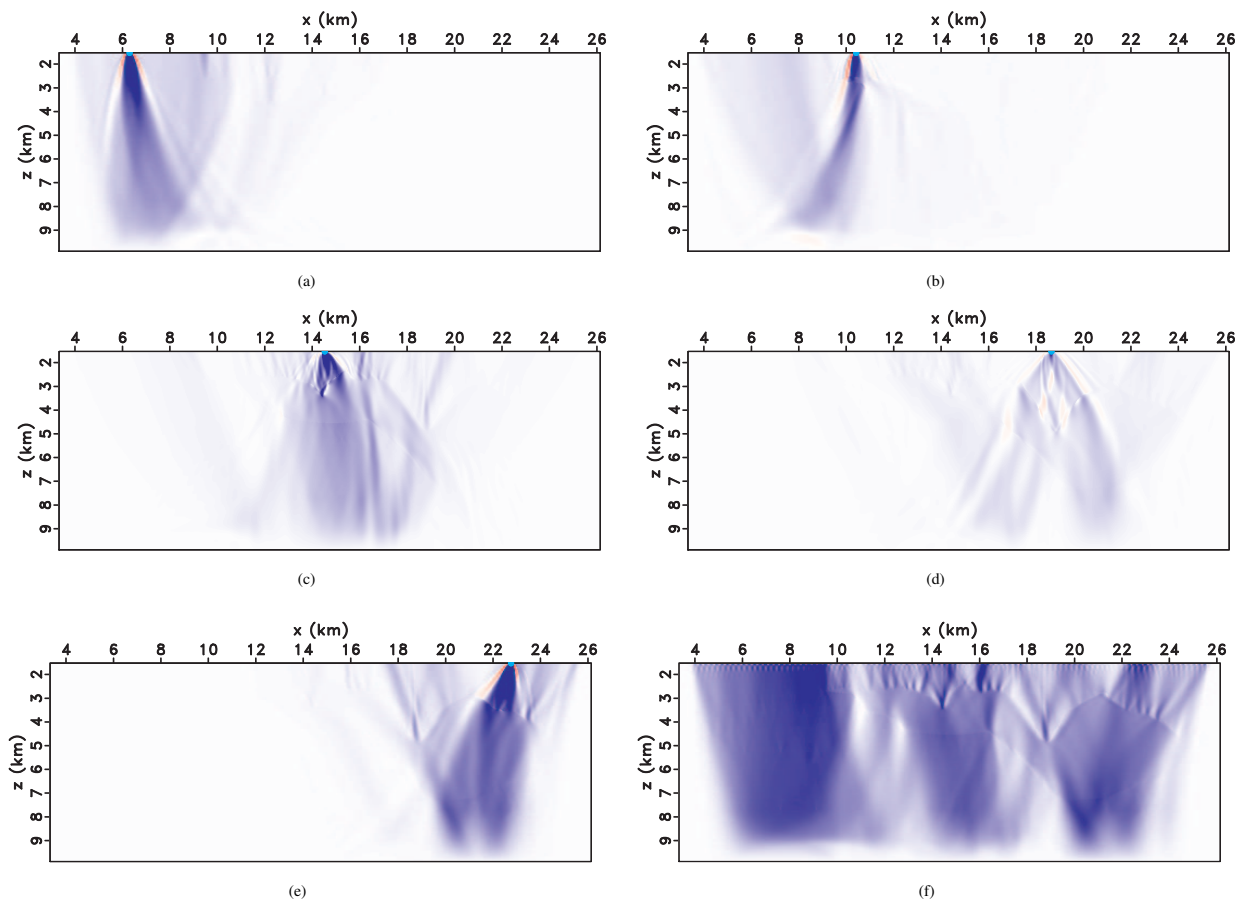


Figure 4: Slowness perturbation obtained from the image perturbation in Figure 3(d) for different shot positions at (a) 6.2 km, (b) 10.2 km, (c) 14.2 km, (d) 18.2 km and (e) 22.2 km. (f) Stacked slowness perturbation corresponding to all shots.

## Time-lag extended image perturbation

### REFERENCES

- Albertin, U., P. Sava, J. Etgen, and M. Maharramov, 2006, Image differencing and focusing in wave-equation velocity analysis: Presented at the 68th Mtg., Abstracts, Eur. Assoc. Expl. Geophys.
- Berkhout, A. J., 1982, Imaging of acoustic energy by wave field extrapolation: Elsevier.
- Biondi, B., and P. Sava, 1999, Wave-equation migration velocity analysis: 69th Annual International Meeting, SEG, Expanded Abstracts, 1723–1726.
- Bishop, T. N., K. P. Bube, R. T. Cutler, R. T. Langan, P. L. Love, J. R. Resnick, R. T. Shuey, D. A. Spindler, and H. W. Wyld, 1985, Tomographic determination of velocity and depth in laterally varying media: *Geophysics*, **50**, 903–923. (Slide set available from SEG Publications Department).
- Claerbout, J. F., 1985, Imaging the Earth's interior: Blackwell Scientific Publications.
- Higginbotham, J. H., and M. P. Brown, 2008, Wave equation migration velocity focusing analysis: Presented at the 78th Annual International Meeting, SEG, Expanded Abstracts.
- Lafond, C. F., and A. R. Levander, 1993, Migration moveout analysis and depth focusing: *Geophysics*, **58**, 91–100.
- MacKay, S., and R. Abma, 1992, Imaging and velocity estimation with depth-focusing analysis: *Geophysics*, **57**, 1608–1622.
- Paffenholz, J., B. McLain, J. Zaskie, and P. Keliher, 2002, Subsalt multiple attenuation and imaging: Observations from the sigsbee 2b synthetic dataset: 72nd Annual International Meeting, SEG, Expanded Abstracts, 2122–2125.
- Pratt, R. G., 1999, Seismic waveform inversion in the frequency domain, Part 1: Theory and verification in a physical scale model: *Geophysics*, **64**, 888–901.
- Sava, P., 2003, Prestack residual migration in the frequency domain: *Geophysics*, **67**, 634–640.
- Sava, P., and B. Biondi, 2004a, Wave-equation migration velocity analysis - I: Theory: *Geophysical Prospecting*, **52**, 593–606.
- , 2004b, Wave-equation migration velocity analysis - II: Subsalt imaging examples: *Geophysical Prospecting*, **52**, 607–623.
- Sava, P., and S. Fomel, 2006, Time-shift imaging condition in seismic migration: *Geophysics*, **71**, S209–S217.
- Sava, P., and I. Vlad, 2008, Numeric implementation of wave-equation migration velocity analysis operators: *Geophysics*, **73**, VE145–VE159.
- Sirgue, L., and R. Pratt, 2004, Efficient waveform inversion and imaging: A strategy for selecting temporal frequencies: *Geophysics*, **69**, 231–248.
- Stork, C., and R. W. Clayton, 1991, An implementation of tomographic velocity analysis: *Geophysics*, **56**, 483–495.
- Woodward, M. J., 1992, Wave-equation tomography: *Geophysics*, **57**, 15–26.
- Yilmaz, O., and R. E. Chambers, 1984, Migration velocity analysis by wave-field extrapolation: *Geophysics*, **49**, 1664–1674.